

# Heating in Aluminum Electrolytic Strobe and Photoflash Capacitors

by

Sam Parler, Jr.  
Director of R&D  
Cornell Dubilier

Capacitor heating occurs in all aluminum electrolytic capacitor applications where a current is present, since the electrolytic capacitor is a non-ideal capacitor which has resistive and other losses. Generally this heating is undesirable and is often a limit to the life of the capacitor. It is important to understand the heating mechanisms so that life and reliability can be predicted. The models for capacitor heating include a simple model for a single sinusoidal frequency, a more complex model for multiple-frequency (non-sinusoidal) small-signal current, and the special case of large-signal heating such as in photoflash and strobe applications.

## *Familiar Dissipation Model*

In most applications, there is a ripple current at 50 Hz or higher, and the resulting AC voltage is small, generally less than 10% of the DC voltage rating of the capacitor. For these applications, the capacitor can be accurately modeled for purposes of heat calculations by the circuit in Figure 1 below.

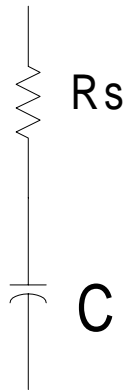


Figure 1: Basic Equivalent Circuit Model of Aluminum Electrolytic Capacitor.

$R_s$  is the familiar ESR as measured on a small-signal capacitance bridge. Neglecting foil and terminal resistance,  $R_s$  can be modeled as

$$R_s = R_{SP}(T) + R_{OX}(f) \quad (1)$$

$$R_{OX} = \frac{DF_{OX}}{2\pi f C} \quad (2)$$

where  $R_{SP}$  is the spacer-electrolyte resistance,  $DF_{OX}$  is the dielectric (aluminum oxide) dissipation factor,  $f$  is the frequency,  $C$  is the capacitance, and  $T$  is temperature. In practice,  $R_{SP}$  varies only with temperature, up to a fairly high frequency at which rolloff begins; this frequency is a function of the foil etch structure and the electrolyte resistivity, which is in turn dependent on composition and temperature.  $DF_{OX}$  is approximately constant at 0.01 to 0.02, and can have some positive or negative temperature coefficient, but is modeled in this paper as constant.

The spacer-electrolyte resistance  $R_{SP}$  is dependent on the electrolyte resistivity, the density and structure of the separator paper, and the dimensions of the paper pad and etched anode surface. The denser and thicker the paper and the higher the electrolyte resistivity, the higher the spacer-electrolyte resistance, but the better the voltage and temperature surge capability. The lower the “gain” (capacitance per unit anode surface area) of the anode foil, the larger the surface area must be to realize a given capacitance, yielding lower  $R_{SP}$ .

Figure 2 shows the relative contributions of the components of  $R_s$  at various temperatures and frequencies.

In applications with small AC voltage ( $V_{PK-PK} < 0.2 \times V_{DC}$ ), if the capacitor's  $R_s$  is known and if the application current and its frequency are known, then the dissipated power can be calculated as

$$P = I^2 R_s \quad (3)$$

and the capacitor temperature can be calculated by taking into account the thermal environment and thermal resistances of the capacitor.

#### Frequency-Distributed Current

When the frequency is distributed, i. e., when the current is not sinusoidal, then the frequency components of the current must be determined by measuring with a spectrum analyzer, by analyzing a digitized current waveform with a computer algo-

rithm, or by using Fourier analysis on a mathematical model of the current waveform. The Fourier analysis procedure is as follows. If the current  $i(t)$  is periodic with period  $\tau$  and is defined on the interval from 0 to  $\tau$  then the Fourier transform  $I(f)$  is defined as

$$I(f) = \sum_{k=-\infty}^{\infty} C_k e^{jf_k t} \quad (4)$$

where  $f_k = 2\pi k/\tau$  and the coefficients  $C_k$  are determined from

$$C_k = \frac{1}{\tau} \int_0^{\tau} i(t) e^{-jf_k t} dt \quad (5)$$

The Fourier analysis can become rather involved, and it's a good idea to do two reality checks after the coefficients have been determined. First, verify that  $C_0 = 0$ , since there can be no DC current

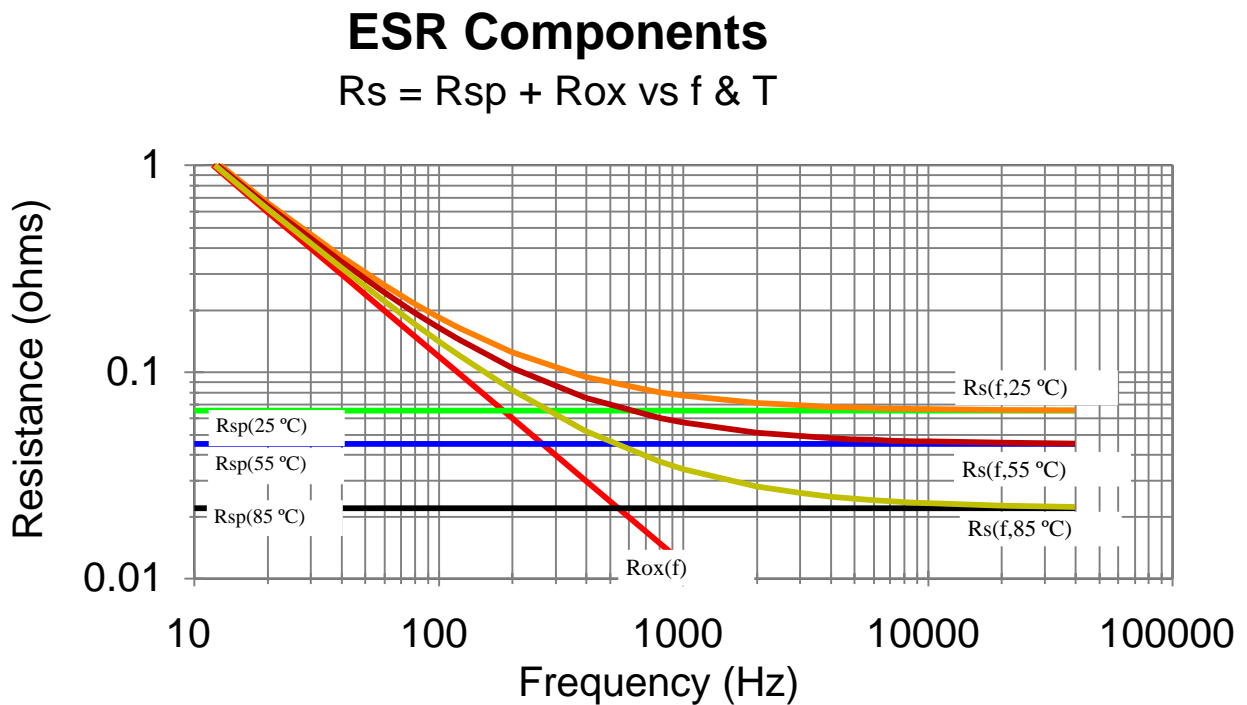


Figure 2:  $R_s$  and its Components for a Typical Capacitor (200  $\mu$ F, 360 V).

in the capacitor without DC leakage current— otherwise it would attempt to store an infinite amount of charge, a physical impossibility. The second check is to verify that the rms current is the same for both the time-distributed current  $i(t)$  and for the frequency-distributed current  $I(f)$ :

$$I_{\text{RMS}} = \sqrt{\frac{1}{\tau} \int_0^{\tau} i^2(t) dt} \quad (6a)$$

$$= \sqrt{\sum_k C_k^2} \quad (6b)$$

After the frequency distribution of the current is determined, then the power is calculated as

$$P_{R_s} = \sum_f I^2(f) R_s(f) \quad (7)$$

An example of a spreadsheet implementation of Fourier analysis is shown in Figure 3 below. This particular example is for a 1000  $\mu\text{F}$ , 400 volt capacitor whose frequency spectrum was measured on a spectrum analyzer.

### *Strobe, Photoflash, and High Ripple Voltage*

The previous model for capacitor dissipation assumes that the  $R_s$  as measured on a small-signal

(1 VAC rms) capacitance bridge can be used to predict heating in capacitors whose AC voltages are higher or lower than 1 volt, and this model is found to be accurate until the AC voltage across the capacitor reaches high levels, as in strobe and photoflash applications.

Strobe capacitors and photoflash capacitors have similar waveforms in their applications, but their designs are quite different due to the repetition rate at which they are designed to operate.

Photoflash capacitors are designed to operate at low rep rates, less than 0.2 Hz, or one flash every 5 seconds. As such, they are usually designed for high energy density,  $> 1 \text{ J/g}$  and  $> 1.5 \text{ J/cc}$ , and a relatively low shot life,  $\leq 100,000$  shots. This is accomplished with crystalline aluminum oxide foils of its high capacitance per surface area. This type of anode structure is not suitable for long life under charge-discharge conditions at voltages above 250 volts, due to mechanical stresses developed in the dielectric crystals.

Strobe capacitors are required to operate at high repetition rates and must therefore exhibit low power loss and high stability for long life ratings,  $> 10$  million shots. This is accomplished by using a low capacitance anode, usually with amorphous aluminum oxide. The open-tunnel structure in the

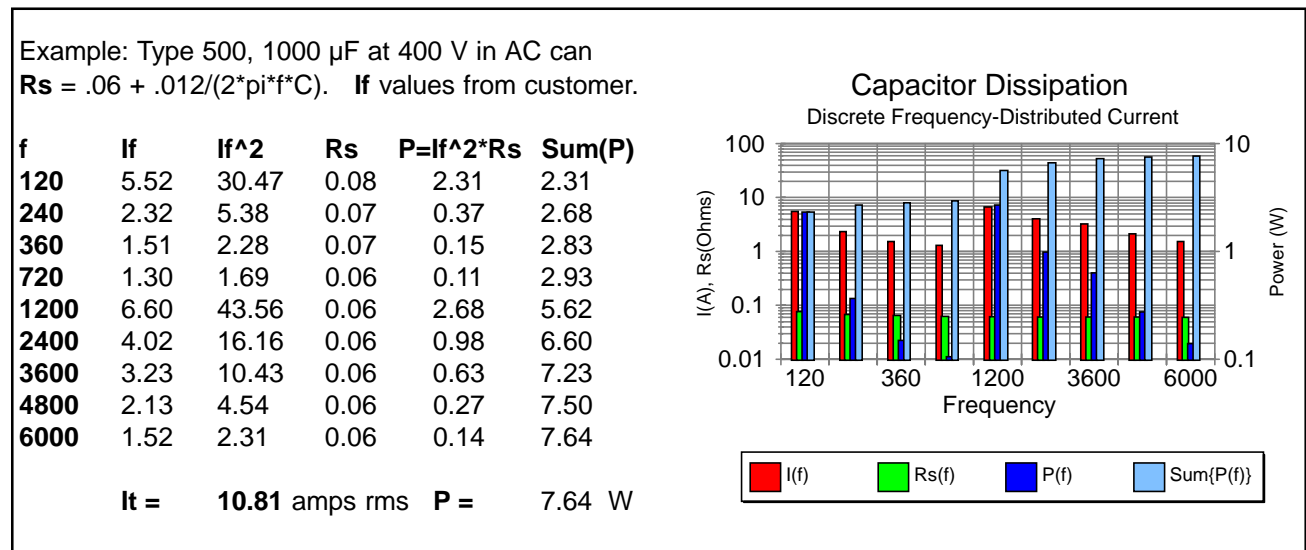


Figure 3: Dissipation Calculation for Frequency-Distributed Current.

anode along with the more flexible dielectric builds up less mechanical stress in the oxide as the capacitor is charged and discharged.

In strobe and photoflash applications, there are several factors which cause the  $I^2R$ s heating model to break down and lose predictive value. First, there is a broad spectrum of frequencies present, so Fourier analysis must be performed. When this is attempted, it is discovered that there is current present at multiples of the frequency of the repetition rate, generally 0.03 to 0.2 Hz for photoflash and 1-5 Hz for strobe.

Many users of strobe capacitors check  $R_s$  on a capacitance bridge at 120 Hz. Unfortunately, this is almost meaningless. Also, effective capacitance during a discharge is generally around 10% higher than the 120 Hz bridge measurement. The slower the dis-

charge or the farther out on the voltage/current “tail” the effective capacitance is measured, the larger the effective capacitance enhancement becomes, due to a complex distribution of dielectric relaxation times.

10-20 Hz is generally the lowest frequency at which a capacitance bridge can perform measurements of  $R_s$ . Nearly all of the resistance at these low frequencies is comprised of the resistance of the aluminum oxide dielectric, and this frequency-varying  $R_s$  component cannot be readily measured at frequencies far below 10 Hz. When analysis is attempted using the measured 10-20 Hz  $DF_{OX}$ , the predicted power dissipation is found to be inaccurate.

Figure 5 on the next page shows a better strobe circuit model. A standard circuit analysis of dissipation proceeds as follows.  $R_c$  is the charge resistance,  $R_d$  is the discharge resistance (ohms),  $V_s$  is the

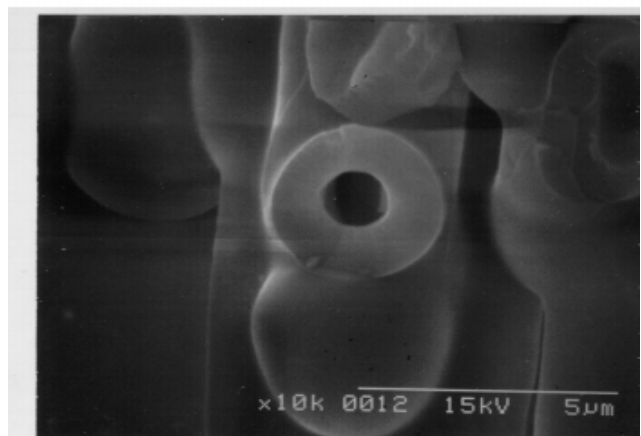
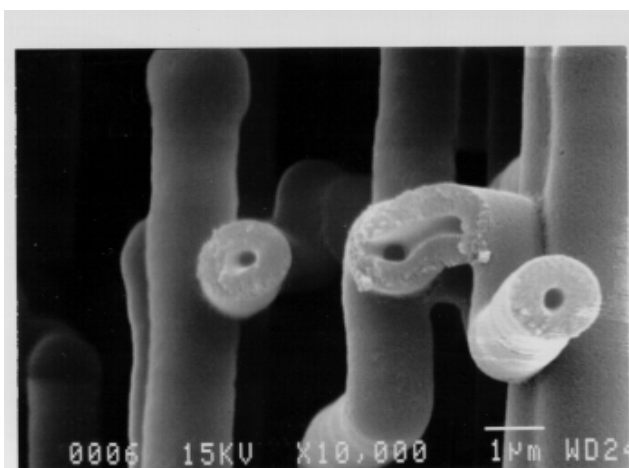
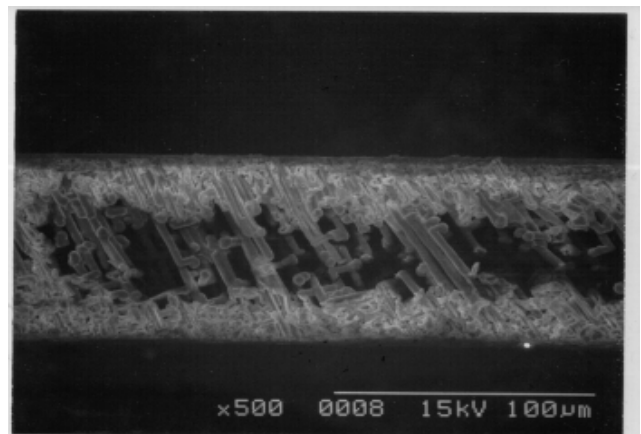
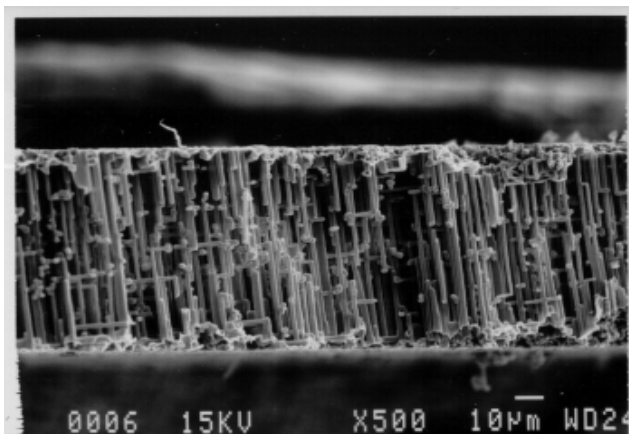


Figure 4: SEM Photos of Photoflash Foil Dielectric (left) and Strobe Foil (right). The aluminum which usually surrounds the dielectric tunnels has been removed for clarity. The dielectric tubes are filled with electrolyte in a working capacitor. Note the difference in foil thickness (top) and tube dimensions (bottom).

power supply voltage (volts), C is the capacitance (farads), and  $R_s$  is the capacitor loss (ohms).  $n$  is defined as the repetition rate (Hz). To determine the power dissipated in the capacitor, the current is separated into charge and discharge portions of the waveform. Assuming S1 is closed at  $t=0$  for a long charge time, much greater than the time constant  $R_c C$ ,

$$i(t) = \frac{V_s}{R_c} e^{-t/R_c C} \quad (8)$$

The energy delivered to  $R_s$  is therefore

$$E'_{R_s} = \int i^2(t) R_s dt \quad (9)$$

Likewise during discharge (S1 open and S2 closed at  $t=T$ ) the current and energy are

$$i(t) = \frac{V_s}{R_d} e^{-(t-T)/R_d C} \quad (10)$$

$$E''_{R_s} = \int i^2(t) R_s dt \quad (11)$$

The total energy dissipated in  $R_s$  per charge-discharge cycle can be shown to be

$$E_{R_s} = \frac{1}{2} C V_s^2 \times \left[ \frac{R_s}{R_s + R_c} + \frac{R_s}{R_s + R_d} \right] \quad (12)$$

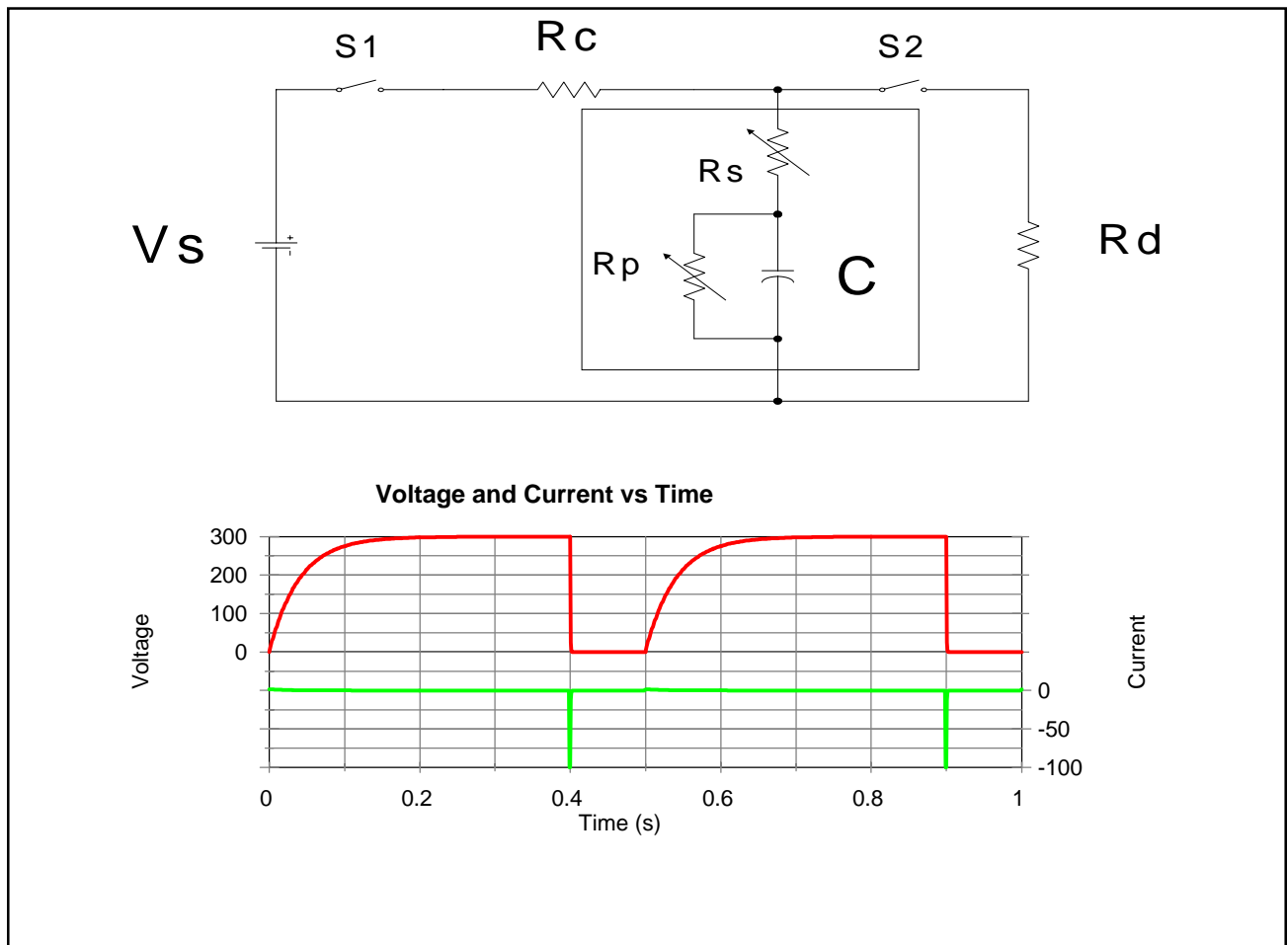


Figure 5: Strobe Circuit Model with Capacitor Model.

Since  $R_c \ll R_d$ , the dissipated energy is very nearly

$$E_{R_s} = \frac{1}{2} C V_s^2 \times \left[ \frac{R_s}{R_s + R_d} \right] \quad (13)$$

The dissipated power at a rep rate of  $n$  Hz is therefore

$$P_{R_s} = \frac{1}{2} n C V_s^2 \times \left[ \frac{R_s}{R_s + R_d} \right] \quad (14)$$

Case temperature rise in still air above ambient temperature is proportional to its dissipated power.

As the current is frequency-distributed, it is not clear what value of  $R_s$  to select, since it depends heavily on frequency. Fourier analysis can be used as shown below in Figure 6 for a  $C=200 \mu\text{F}$  strobe capacitor being charged by a  $V_s=360$  volt DC power supply through an  $R_c=50$  ohm resistor and discharged into an  $R_d=1$  ohm load resistor at an  $n=2$  Hz rep rate.  $R_{sp}$  and  $D_{fox}$  are chosen to fit bridge measurements. The analysis is checked for validity through the computation of rms current in the time and frequency domains (equation 6), 5.145 vs 5.010 amps. These are within 3% so most likely no gross math errors have been made. A dissipated power of 3.88 watts from a stored energy of 12.96 joules is calculated. An effective ESR of 0.155 ohms is calculated. This indicates that about 15% of the stored energy is lost as heat.

ESR modeling and Fourier analysis were performed for two different 200  $\mu\text{F}$ , 360 volt strobe capacitors of approximately the same size and weight. One unit was produced by a well-known Japanese manufacturer (unit "R") and the other, slightly smaller and lighter unit was produced by Cornell Dubilier (unit "C"). Unit R had apparently been optimized for low ESR, as its ESR was about 20-30% lower than that of unit C at all temperatures and frequencies. In addition, the dielectric dissipation factor of unit R was also much lower than that of unit C, and, unlike unit C, its oxide DF had the supposedly desirable property of diminishing with increasing temperature. Unit C had been optimized for robustness against high voltage and high temperature excursions, and had been optimized for strobe performance. The leakage current of the two units were similar.

Strobe test stand data were taken for a wide variety of load conditions (Figure 7). Rep rate was varied from 0.5 to 5 Hz; discharge resistance was used at 0.5, 1.0, and 2.0 ohms; and voltage was varied from 200 volts to 360 volts. Contrary to any known dissipation model predictions, unit C, *the capacitor with the higher ESR, was found to run cooler, with lower power dissipation*, than unit R, in almost every test condition. It is possible that unit R sacrificed strobe performance to obtain lowest ESR for some customers who judged quality by that criterion alone.

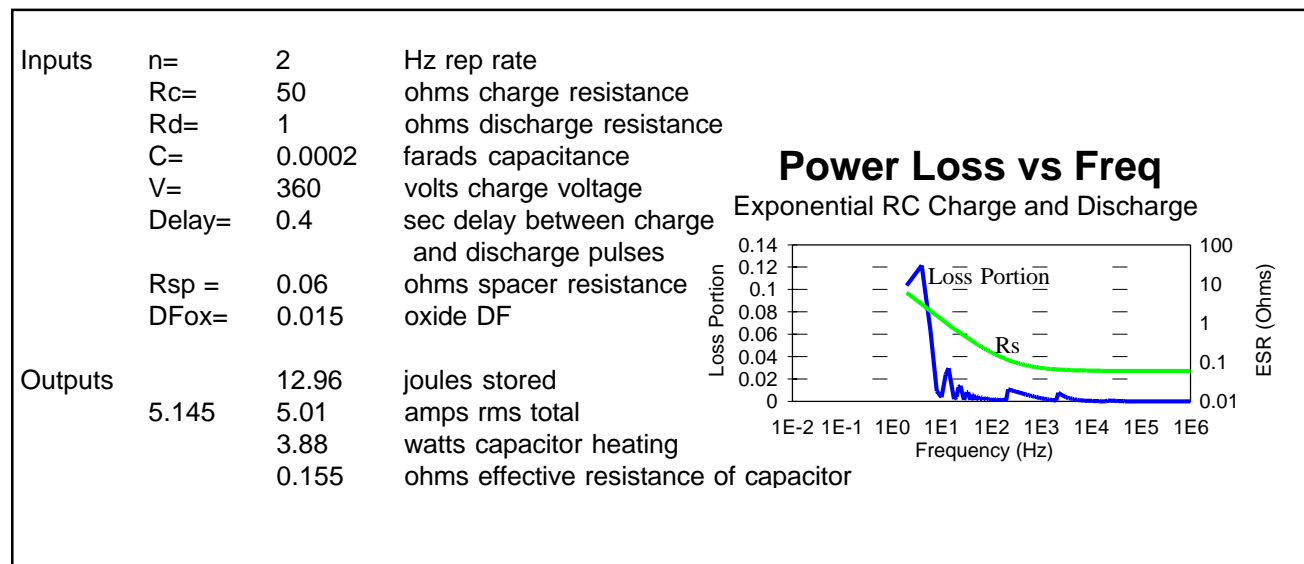


Figure 6: Fourier Analysis used in Predicting Strobe Capacitor Performance.

No thermal model existed until recently for predicting power dissipation and case temperature for capacitors used in strobe tests. It is clear that no model based on an ESR and Fourier analysis alone would be sufficient.

The reason for the inaccuracy of ESR models in predicting strobe capacitor power dissipation and case temperature is that it does not take into account observed dielectric absorption behavior, which causes the dissipated power to be less than linear with repetition rate, and AC voltage coefficient of dielectric loss. These phenomena have been investigated and reported in the literature by this author and others.

### Rs-Cycle Power Model for Strobe Capacitors

Any accurate power loss model should be based on real and observed dissipation mechanisms. We know that the spacer-electrolyte resistance  $R_{sp}$  is present and acts in series with the dielectric. This series resistance is truly in series with the dielectric in that it limits the achievable peak current and discharge time. The remainder of the power acts from within the dielectric system, so that it can be thought of as a non-ohmic loss occurring in parallel with the capacitor. This non-ohmic power loss has been observed to be a function of voltage, dielectric composition, and dielectric structure. It appears to be related to frictional loss due to mechanical strain within the dielectric.

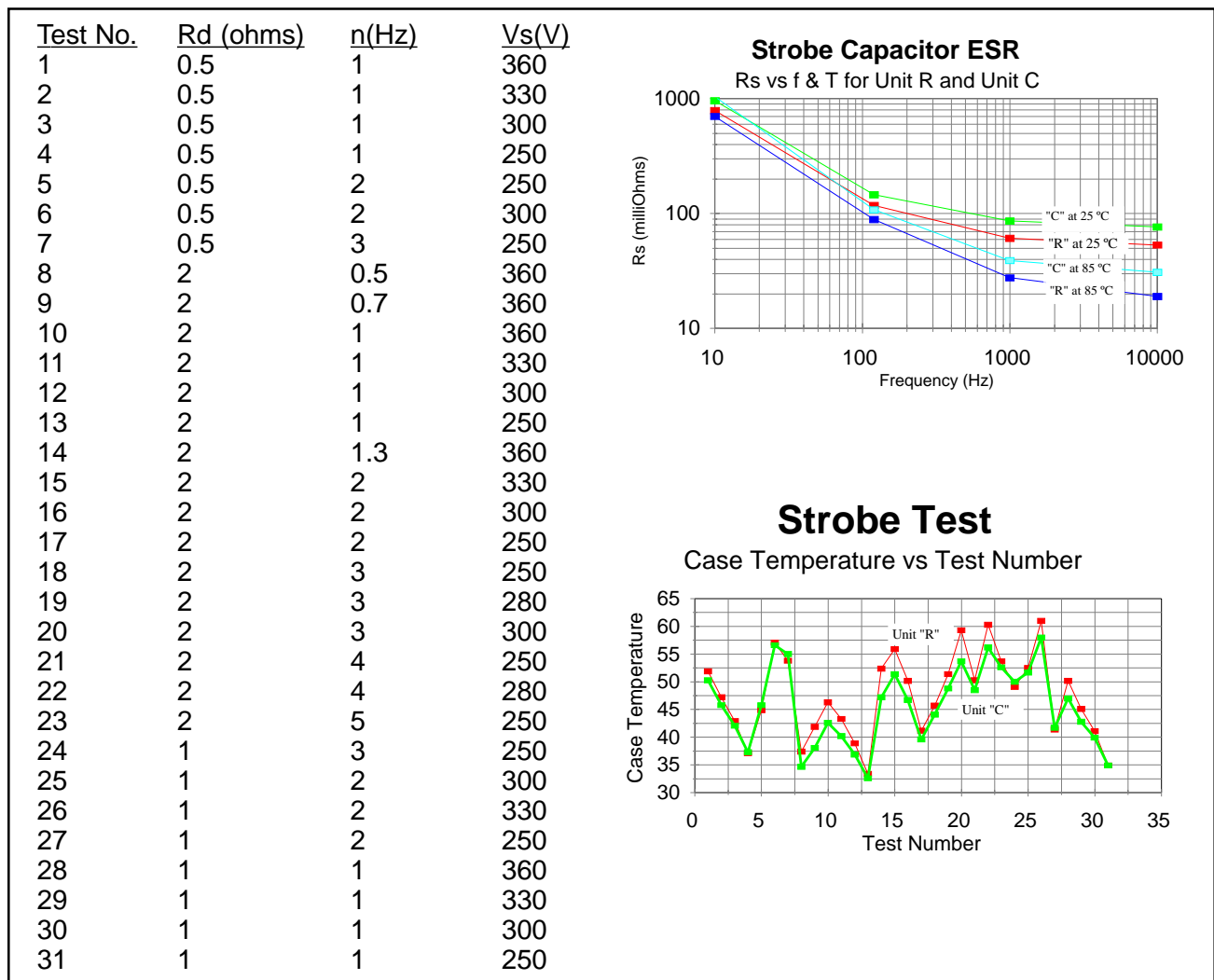


Figure 7: Comparison of ESR and Strobe Performance for Units “R” and “C”.

Figure 8 below compares the behavior of an aluminum electrolytic capacitor during a constant-current charge-discharge cycle. This is especially interesting because the waveforms for an ideal capacitor are linear and deviations from theoretical are readily observed by a visual inspection. The waveforms were captured on a digital oscilloscope with 12-bit vertical resolution, and the  $dV/dt$  measurements and graph were made with the built-in digital math functions of the oscilloscope.

For an ideal capacitor charged with a constant current  $I_c$  beginning at time  $t=0$ , the voltage across the capacitor should rise linearly with time:

$$V_c = I_c \times t \quad (15)$$

The slope of the charge voltage is constant:

$$\frac{dV_c}{dt} = I_c \quad (16)$$

Even if the capacitor has a constant series resistive loss as modeled as  $R_s$  in Figure 1, the capacitor

voltage would still be linear in time. Observing the waveforms below in Figure 8, this is clearly not the case. The slope of the capacitor voltage during charge is less than that of an ideal capacitor, and the voltage waveform is concave downward. One might be tempted to attribute this to leakage current or a parallel loss mechanism, but during the discharge portion, the voltage also diminishes less than an ideal capacitor, implying that some of the excess current passed through the capacitor during the charge cycle is recovered during the discharge.

The unrecovered energy during such a charge-discharge cycle was calculated directly in the time domain by integrating the instantaneous capacitor power, which is simply the product of the capacitor voltage and current. This unrecovered energy is seen below.

Additional investigations into this anomalous behavior of aluminum electrolytic capacitors during charge-discharge have led to a preliminary semi-empirical power loss model.

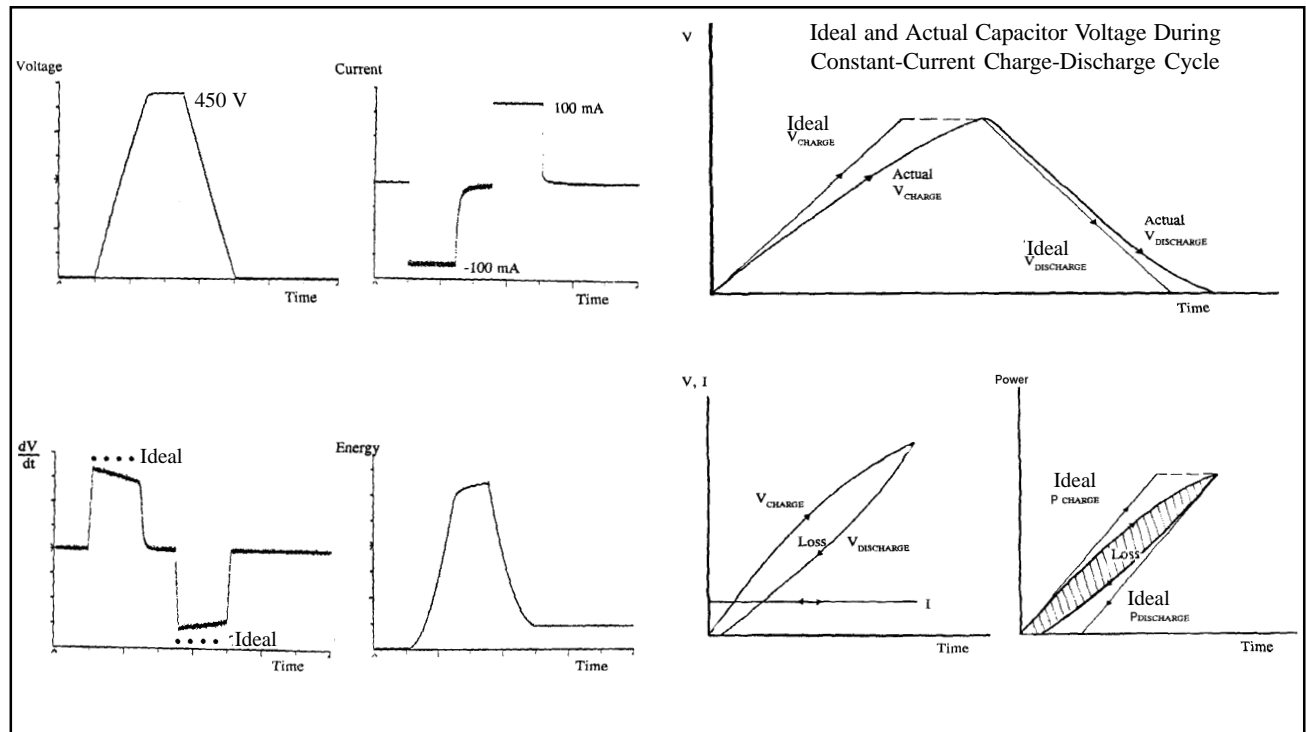


Figure 8: Waveforms of Typical Aluminum Electrolytic Capacitor During Constant Current Charge/Discharge Cycling. The four waveforms on the left are from a digital storage oscilloscope, and the three exaggerated diagrams on the right illustrate the hysteresis energy loss during the cycle.

The Rs-Cycle power loss model for strobe and photoflash capacitors is comprised of two mathematical terms, one representing the series loss due to Rsp and the other representing the loss suggested by Rp in Figure 5. This loss includes both the dielectric loss due to the dissipation factor as well as cycle losses due to the impression of AC voltage upon the dielectric.

The model is

$$P = \frac{1}{2}CV^2 \times \left[ \frac{nR_{sp}}{R_{sp} + R_d} + Bn^G \times V^D \right] \quad (17)$$

and

$$\Delta T = \theta \times P \quad (18)$$

where:

- $\Delta T$  = Heat rise above ambient (°C)
- $\theta$  = Thermal resistance of case to air (°C/W)
- C = Capacitance (F)
- P = Dissipated power (W)
- n = rep rate (Hz)
- Rsp = Series spacer-electrolyte resistance (Ω)
- Rd = Discharge load resistance (Ω)
- V = Operating voltage (V)

- B = Cycle loss factor [Hz<sup>(1-G)</sup> × V<sup>(-D)</sup>]
- D = Voltage exponent of heat loss (unitless)
- G = Rep rate exponent of heat loss (unitless)

Unfortunately, the parameters of B, D, and G vary somewhat with different capacitor designs, and there is no known way to predict or determine these values until strobe data is taken.

Once the parameter values are known, however, the Rs-Cycle model is predictive of AC heating under new test conditions.

A typical Rs-Cycle model is shown along with the test data below in Figure 9. The fit is generally accurate to within 1 °C.

Further refinements to this model would include temperature compensation of Rsp and of the dielectric loss portion.

As one final word of caution, initial heating alone is not the only issue in strobe and photoflash performance. Just as important is the stability of this heating: Does the case temperature increase during a life test, and if so, at what rate? Also, the rate of internal gassing and pressure build-up is important, as even a cool capacitor will generally not last long once its safety vent seal is compromised.

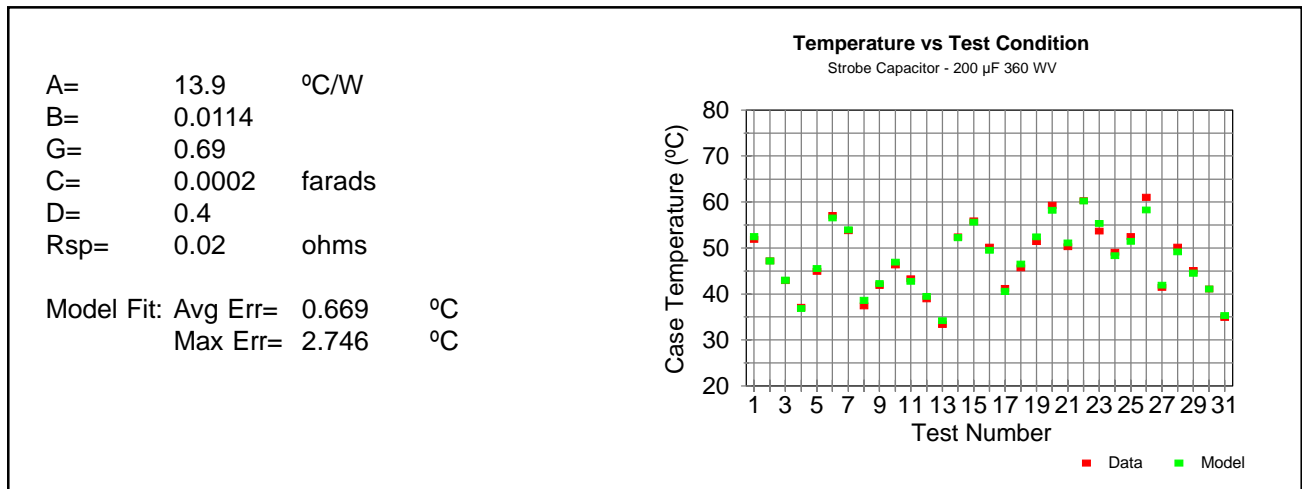


Figure 9: Rs-Cycle Semi-empirical Dissipation Model Fit to Actual Strobe Data.

## BIBLIOGRAPHY

1. S. G. Parler, Jr. and J. W. Dieter, "Aluminum Electrolytic Capacitors for Repetition Rated Discharge", Tech. Report DNA-TR-90-191, Defense Nuclear Agency contract DNA-001-87-C-0098 (1991).
2. R. S. Alwitt and S. G. Parler, Jr., "Heat Generation During Pulse Operation of Prototype Aluminum Electrolytic Capacitors", *J. Applied Electrochemistry* **25** (1995) 533-542.
3. R. S. Alwitt, "Charge/Discharge Characteristics of Prototype Aluminum Electrolytic Capacitors", presented at the IEEE Industry Applications Society Meeting, New Orleans, Oct. 5-9, 1997.
4. J. L. Ord, "Electrostriction in Anodic Oxides: Exchange of Elastic and Electrostatic Energy", *J. Electrochemical Society* **138**, 2934 (1991).
5. J. L. Ord and W. P. Wang, "Optical Anisotropy and Electrostriction in the Anodic Oxide of Tantalum", *J. Electrochemical Society* **130**, 1809 (1983).
6. H. Kliem, H. Kraus, and G. Arlt, "Non-linear Dielectric Relaxation in High Electric Fields", *Int. Conf. Appl. Diel. Mat.* 1985, pp. 110-113 (1985).
7. R. S. Alwitt and T. Hasebe, "Factors Contributing to Energy Loss of Electrolytic Capacitors During Charge/Discharge Operation", presented at CARTS '98 (Capacitor and Resistor Technology Symposium), March 9-12, 1998.